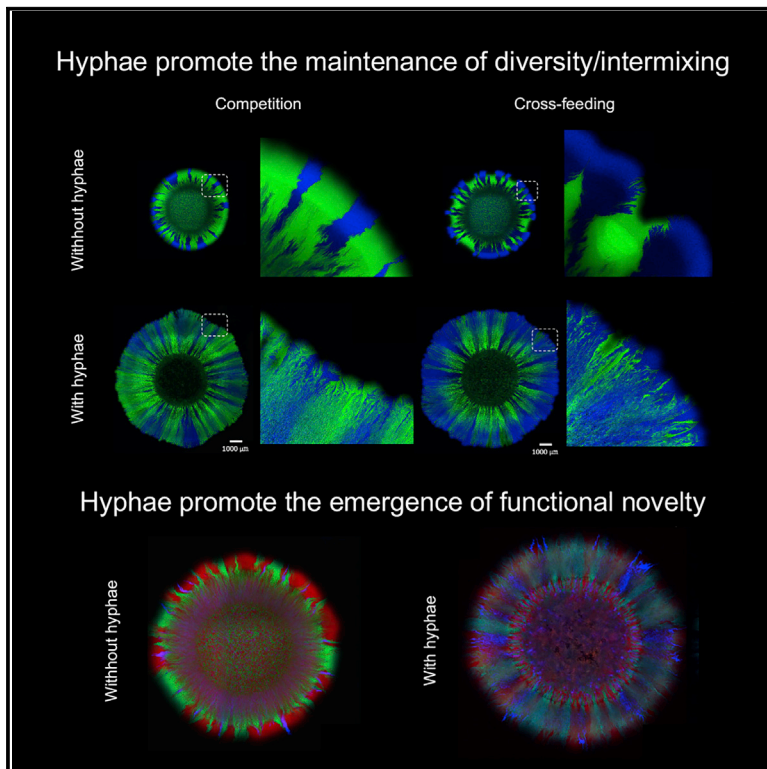


## Fungal hyphae regulate bacterial diversity and plasmid-mediated functional novelty during range expansion

### Graphical abstract



### Authors

Chujin Ruan, Josep Ramoneda,  
Guram Gogia, Gang Wang,  
David R. Johnson

### Correspondence

david.johnson@eawag.ch (D.R.J.),  
gangwang@cau.edu.cn (G.W.)

### In brief

Ruan et al. demonstrate that fungal hyphae can promote and maintain bacterial diversity during range expansion. Fungal hyphae increase bacterial dispersal, which counteracts the effects of ecological drift at the expansion frontier. This increases the spatial intermixing of different populations and promotes plasmid-mediated functional novelty.

### Highlights

- Fungal hyphae promote and maintain bacterial diversity during range expansion
- Fungal hyphae increase bacterial dispersal and counteract ecological drift
- This increases the spatial intermixing of different bacterial populations
- The increased spatial intermixing promotes plasmid-mediated functional novelty



## Article

# Fungal hyphae regulate bacterial diversity and plasmid-mediated functional novelty during range expansion

Chujin Ruan,<sup>1,2,7</sup> Josep Ramoneda,<sup>2,3,7</sup> Guram Gogia,<sup>2,4</sup> Gang Wang,<sup>1,5,\*</sup> and David R. Johnson<sup>2,6,8,\*</sup><sup>1</sup>College of Land Science and Technology, China Agricultural University, 100193 Beijing, China<sup>2</sup>Department of Environmental Microbiology, Swiss Federal Institute of Aquatic Science and Technology (Eawag), 8600 Dübendorf, Switzerland<sup>3</sup>Cooperative Institute for Research in Environmental Sciences, University of Colorado, Boulder, CO 80309, USA<sup>4</sup>Department of Environmental Systems Science, Swiss Federal Institute of Technology, 8092 Zürich, Switzerland<sup>5</sup>National Black Soil & Agriculture Research, China Agricultural University, 100193 Beijing, China<sup>6</sup>Institute of Ecology and Evolution, University of Bern, 3012 Bern, Switzerland<sup>7</sup>These authors contributed equally<sup>8</sup>Lead contact

\*Correspondence: david.johnson@eawag.ch (D.R. J.), gangwang@cau.edu.cn (G. W.)

<https://doi.org/10.1016/j.cub.2022.11.009>**SUMMARY**

The amount of bacterial diversity present on many surfaces is enormous; however, how these levels of diversity persist in the face of the purifying processes that occur as bacterial communities expand across space (referred to here as range expansion) remains enigmatic. We shed light on this apparent paradox by providing mechanistic evidence for a strong role of fungal hyphae-mediated dispersal on regulating bacterial diversity during range expansion. Using pairs of fluorescently labeled bacterial strains and a hyphae-forming fungal strain that expand together across a nutrient-amended surface, we show that a hyphal network increases the spatial intermixing and extent of range expansion of the bacterial strains. This is true regardless of the type of interaction (competition or resource cross-feeding) imposed between the bacterial strains. We further show that the underlying cause is that flagellar motility drives bacterial dispersal along the hyphal network, which counteracts the purifying effects of ecological drift at the expansion frontier. We finally demonstrate that hyphae-mediated spatial intermixing increases the conjugation-mediated spread of plasmid-encoded antibiotic resistance. In conclusion, fungal hyphae are important regulators of bacterial diversity and promote plasmid-mediated functional novelty during range expansion in an interaction-independent manner.

**INTRODUCTION**

Surface-associated bacterial communities are ubiquitous across our planet and have important roles in biogeochemical cycles, ecosystem processes, agriculture, environmental sustainability, and human health and disease.<sup>1–3</sup> A universal feature of all communities is that they must, at some point in their existence, undergo range expansion.<sup>4,5</sup> Range expansion refers to the spreading of organisms across space as a consequence of their reproduction and dispersal. During the range expansion process, communities undergo irreversible diversity loss due to small effective population sizes and strong ecological drift at the expansion frontier, where only a few individuals positioned at the frontier contribute to further range expansion.<sup>4–9</sup>

The universality of range expansion and its associated negative effects on the maintenance of diversity raises an important paradox. Many surface-associated bacterial communities are incredibly diverse, where soil and host-associated microbiomes may contain many hundreds to thousands of bacterial taxa.<sup>10–12</sup> How are these levels of bacterial diversity maintained in the face of the purifying effects that occur during range expansion?

Resource cross-feeding between cell-types is one process that can counteract these effects, where cross-feeding tends to maintain higher levels of spatial intermixing of different cell-types and thus higher levels of diversity.<sup>13–15</sup> However, cross-feeding does not universally occur between all bacterial cell-types; rather, competition is also pervasive.<sup>16–18</sup> Are there mechanisms that counteract the purifying effects of ecological drift at the expansion frontier that are independent of interactions? Resource supply,<sup>19</sup> metabolite toxicity,<sup>20</sup> initial cell densities,<sup>21</sup> initial spatial configurations of cells,<sup>22,23</sup> and spatial structure<sup>24</sup> can all affect short-term spatial intermixing during range expansion in an interaction-independent manner, but they either have no effects on long-term spatial intermixing or have effects that are too small to account for the levels of diversity observed in nature. In spatially heterogeneous environments such as soils or the gut lumen, spatial isolation maintains diversity by preventing competitive exclusion of populations.<sup>25</sup> However, at the scale of each isolated population, the effects of drift during proliferation are still expected to negatively impact diversity. Clearly, further knowledge on the processes that maintain bacterial diversity during range expansion is needed to resolve this paradox.



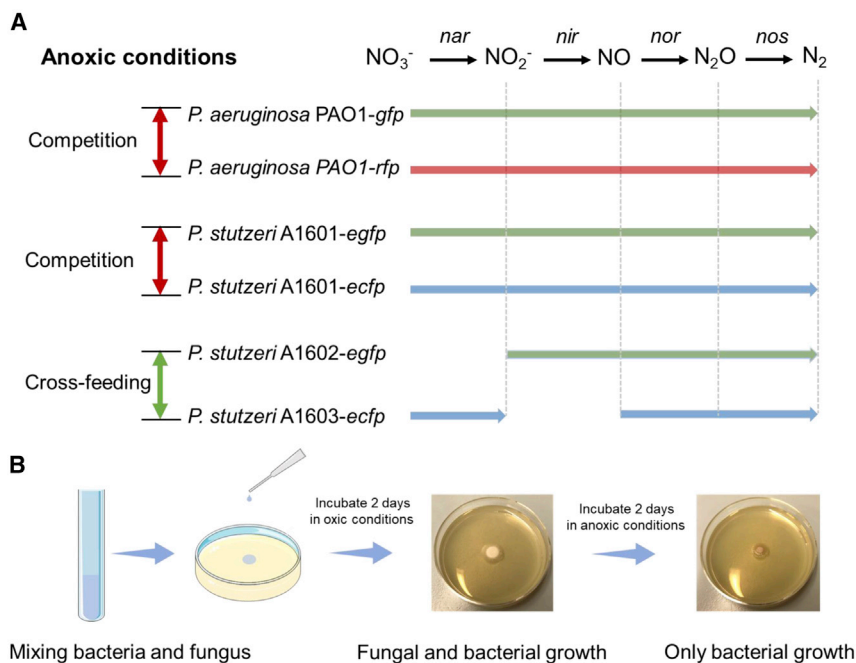


**Figure 1. Experimental system and approach**

(A) Our experimental system consists of pairs of isogenic mutant strains of *P. aeruginosa* or *P. stutzeri*. The competing strains of *P. aeruginosa* PAO1-*gfp* and PAO1-*rfp* and *P. stutzeri* A1601-*egfp* and A1601-*ecfp* can completely reduce nitrate ( $\text{NO}_3^-$ ) to nitrogen gas ( $\text{N}_2$ ) when grown in an anoxic environment with an exogenous supply of nitrate. They express different fluorescent proteins but are otherwise genetically and phenotypically identical. The cross-feeding strains of *P. stutzeri* A1602-*egfp* and A1603-*ecfp* have single loss-of-function deletions in different steps of the denitrification pathway that cause them to cross-feed nitrite ( $\text{NO}_2^-$ ) when grown in an anoxic environment with an exogenous supply of nitrate. Nar, nitrate reductase; Nir, nitrite reductase; Nor, nitric oxide reductase; Nos, nitrous oxide reductase. Thick colored arrows indicate the metabolic processes performed by each strain and the color of the respective chromosomally encoded fluorescent protein that they express (green, red, or cyan fluorescent protein).

(B) We mixed pairs of the bacterial strains with *Penicillium* sp. laika and inoculated the mixtures onto the surfaces of nutrient-amended agar plates. We first incubated the agar plates in oxic conditions to promote the development of a hyphal network.

We then incubated them in anoxic conditions to stop growth of *Penicillium* sp. laika and allow the bacteria to grow and disperse according to their anoxia-induced interactions (competition or cross-feeding). We performed control experiments without *Penicillium* sp. laika in otherwise identical experiments. See also Figure S1.

We hypothesized here that bacterial dispersal via fungal hyphae can counteract the purifying effects of ecological drift at the expansion frontier during range expansion in an interaction-independent manner. Bacteria and fungi co-occur in a myriad of environments, including soils,<sup>26</sup> host-associated microbiomes,<sup>27–30</sup> and a variety of biotechnological applications.<sup>31</sup> Importantly, fungal hyphae can promote bacterial dispersal on virtually any surface where they co-occur, where the water films surrounding fungal hyphae provide hydrated environments that enable active bacterial motility.<sup>32–37</sup> This, in turn, has important consequences for the functioning of surface-associated bacterial communities, where increased bacterial dispersal can improve access to growth resources,<sup>38–40</sup> promote conjugation-mediated plasmid transfer,<sup>41</sup> enable escape from predators,<sup>42</sup> and promote transport of phages.<sup>43</sup> Although not established for fungal hyphae, dispersal and its trade-offs with growth rate can promote the maintenance of diversity by reducing interspecific competition.<sup>44–49</sup> Together, this evidence suggests that increased bacterial dispersal along fungal hyphae could help resolve the paradox between observed levels of surface-associated bacterial diversity and the universal processes that drive diversity loss during range expansion.

To test our hypothesis, we performed range expansion experiments with pairs of bacterial strains in the presence or absence of a hyphae-forming fungus. We expected that the thin water-film networks surrounding fungal hyphae would serve as dispersal pathways that allow bacteria to escape the effects of ecological drift at the expansion frontier and occupy uncolonized space, leading to higher spatial intermixing. Higher spatial intermixing indicates higher bacterial diversity, as more individuals

are able to emigrate from the founder population and contribute to active range expansion.<sup>7,15,20</sup> We next tested whether the effects of fungal hyphae on spatial intermixing are independent of the type of interaction imposed between the bacterial strains (competition or resource cross-feeding). We then tested defects in pili- and flagella-mediated motility to identify the active dispersal mechanism along fungal hyphae. Finally, we addressed the consequences of hyphae-mediated spatial intermixing on the spread of plasmid-encoded functional novelty, with specific focus on the spread of antibiotic resistance.

## RESULTS

### Fungal hyphae counteract the loss of spatial intermixing of competing bacterial strains during range expansion

We first tested whether the presence of fungal hyphae can counteract the loss of spatial intermixing of competing bacterial strains during range expansion and thus counteract the loss of bacterial diversity. To test this, we used two pairs of competing bacterial strains (*Pseudomonas aeruginosa* PAO1-*gfp* and PAO1-*rfp*, and *Pseudomonas stutzeri* A1601-*egfp* and A1601-*ecfp*), where each strain expresses a different fluorescent protein but is otherwise genetically and phenotypically identical to its paired strain (Figure 1A; Table S1). Both strains have the complete denitrification pathway and will compete for nitrate ( $\text{NO}_3^-$ ) when grown together under anoxic conditions with an exogenous supply of nitrate. We conducted experiments where we mixed the pairs either with or without the hyphae-forming fungus *Penicillium* sp. laika and inoculated them onto agar plates amended with nitrate (Figure 1B). We next incubated the agar

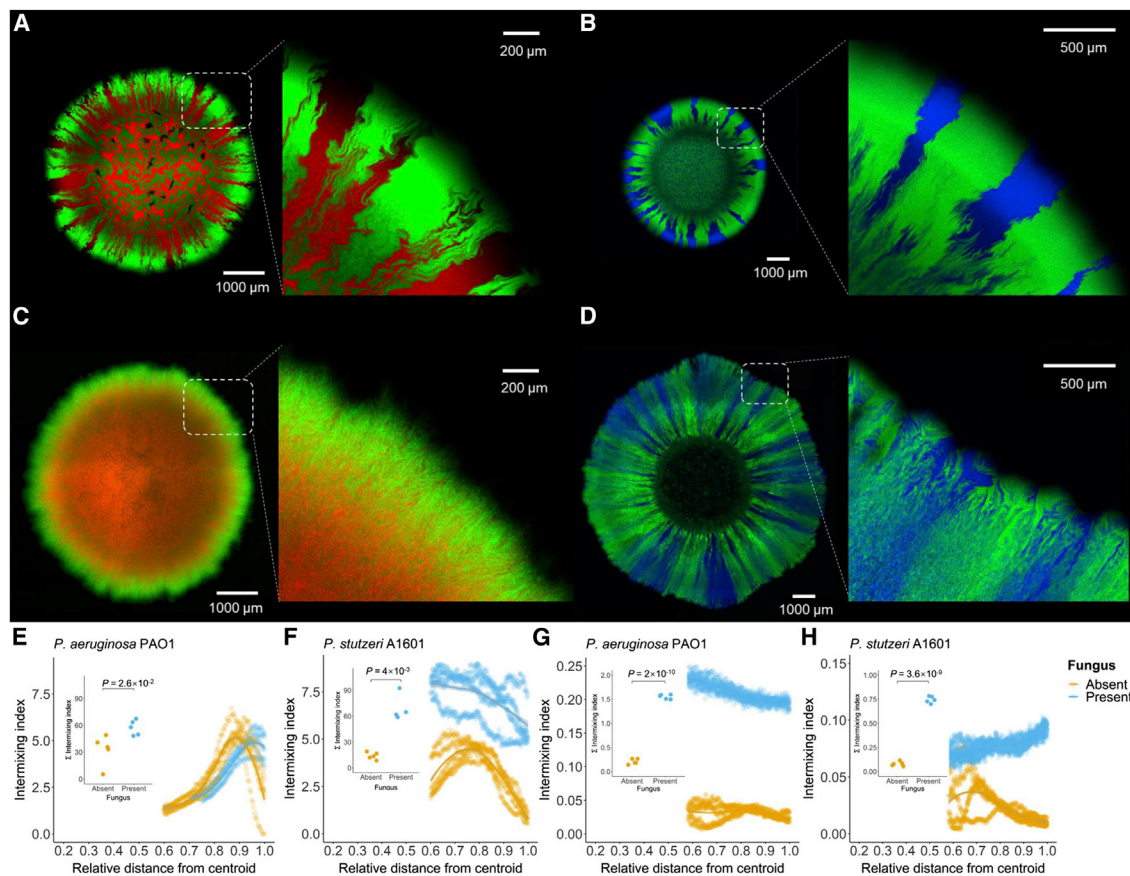


**Figure 2. Range expansions of competing bacterial strains in the absence or presence of fungal hyphae**

(A–D) Representative images after 4 days of range expansion in the (A and B) absence or (C and D) presence of *Penicillium* sp. laika. Images are for the competing pair of (A and C) *P. aeruginosa* PAO1 or (B and D) *P. stutzeri* A1601 strains.

(E–H) Quantification of the intermixing index using the local-scale Fourier transform method as a function of distance from the centroid for the competing pair of (E) *P. aeruginosa* PAO1 or (F) *P. stutzeri* A1601 strains. Quantification of the intermixing index using the intersection method as a function of distance from the centroid for the competing pair of (G) *P. aeruginosa* PAO1 or (H) *P. stutzeri* A1601 strains. We quantified the intermixing index in the radial direction from the outer edge of the inoculation area to the outer edge of the final expansion frontier at the end of the range expansion experiment. The insets depict the intermixing indices at the expansion frontier (35  $\mu\text{m}$  band from the expansion edge). This intermixing index is the sum of indices at increments of 5  $\mu\text{m}$  across the 35  $\mu\text{m}$ -wide frontier. The lines are the moving averages of the intermixing index. Each data point is the measurement for an independent experimental replicate ( $n = 5$ ) and  $p$  is for a two-sample two-sided Welch test.

See also Figures S2–S5.

plates for 2 days under oxic conditions (Figure 1B), which allowed the fungus to form a dense hyphal network (Figure S1A) and the bacterial strains to begin growing and dispersing across the hyphal network (Figure S1B). We finally transferred the agar plates to anoxic conditions to induce nitrate competition between the bacterial strains and incubated them for an additional 2 days (Figure 1B). The fungus could not grow under anoxic conditions (Figure S1C), whereas the bacterial strains could continue growing with nitrate and disperse across the hyphal network.

Consistent with our expectation, we found that the presence of fungal hyphae can indeed counteract the loss of spatial intermixing between competing bacterial strains at the expansion frontier (Figure 2). Here and throughout, we defined the expansion frontier as a 35  $\mu\text{m}$ -wide band located at the leading edge of the expansion area, which reflects growth during the anoxic phase and was selected based on experimental measures of the width of the actively growing layer of bacterial cells in similar

experimental setups.<sup>19</sup> For the *P. aeruginosa* PAO1 strains, the presence of fungal hyphae significantly increased spatial intermixing at the expansion frontier (two-sample two-sided Welch tests;  $p < 0.03$ ,  $n = 5$ ) (Figures 2E [local-scale Fourier transform method] and 2G [intersection method]), an effect that progressively weakened at increasing distances behind the expansion frontier (Figures S2A [local-scale Fourier transform method] and S3A [intersection method]). The increase in intermixing by fungal hyphae was further amplified when we quantified intermixing at intermediate scales (Figure S4), but we focused here on the local scale as this scale operates closest to the finest scales of intermixing that we observed experimentally. For the *P. stutzeri* A1601 strains, fungal hyphae also significantly increased spatial intermixing at the expansion frontier (two-sample two-sided Welch tests;  $p < 0.004$ ,  $n = 5$ ) (Figures 2F [local-scale Fourier transform method] and 2H [intersection method]), and this effect persisted across the entire expansion area

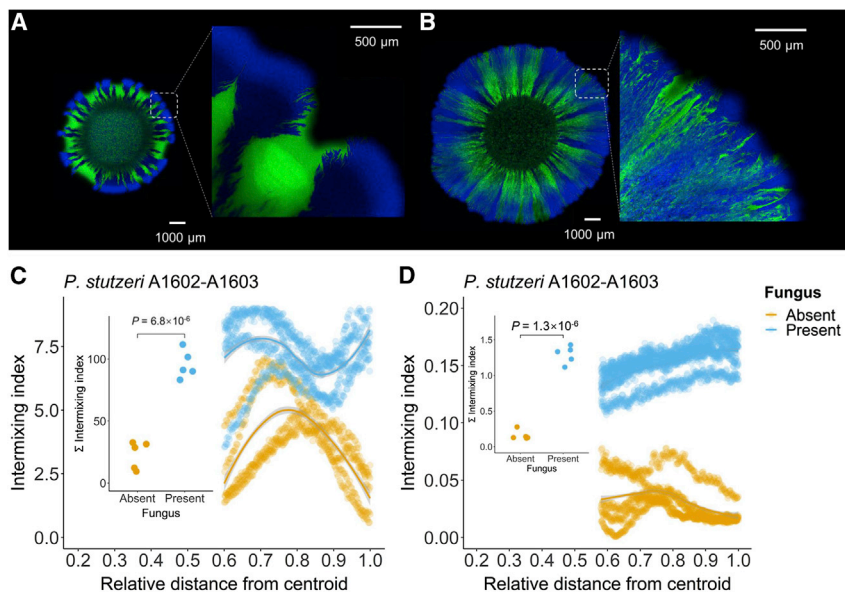


**Figure 3. Range expansions of cross-feeding bacterial strains in the absence or presence of fungal hyphae**

(A and B) Representative images of the cross-feeding pair of *P. stutzeri* A1602 and A1603 strains after 4 days of range expansion in the (A) absence or (B) presence of *Penicillium* sp. laika.

(C) Quantification of the intermixing index using the local-scale Fourier transform method as a function of distance from the centroid.

(D) Quantification of the intermixing index using the intersection method as a function of distance from the centroid.

For (C) and (D), we quantified the intermixing index in the radial direction from the outer edge of the inoculation area to the outer edge of the final expansion frontier at the end of the range expansion experiment. The inset depicts the intermixing index at the expansion frontier (35  $\mu\text{m}$  band from the expansion edge). This intermixing index is the sum of indices at increments of 5  $\mu\text{m}$  across the 35  $\mu\text{m}$ -wide frontier. The lines are the moving averages of the intermixing index. Each data point is the measurement for an independent experimental replicate ( $n = 5$ ) and  $p$  is for a two-sample two-sided Welch test.

See also Figures S2–S5.

(Figures S2B [local-scale Fourier transform method] and S3B [intersection method]).

We further found that the presence of fungal hyphae increased consortium-level expansion distances of competing bacterial strains (Figures S5A and S5B). The expansion radii were significantly greater in the presence of fungal hyphae than in the absence for both pairs of bacterial strains (two-sample two-sided Welch tests;  $p = 0.02$  for the *P. aeruginosa* PAO1 pair,  $p = 1 \times 10^{-8}$  for the *P. stutzeri* A1601 pair,  $n = 5$ ) (Figures S5A and S5B). This could be caused either by improved dispersal or improved growth of the bacterial strains when in the presence of fungal hyphae. To discriminate between these two possibilities, we quantified the total biomass of the pairs of competing bacterial strains when in the presence or absence of fungal hyphae at the end of the range expansion experiment. For the *P. aeruginosa* PAO1 strains, the total biomass was statistically identical when in the presence or absence of fungal hyphae (two-sample two-sided Welch test;  $p = 0.07$ ,  $n = 5$ ) (Figure S5D). For the *P. stutzeri* A1601 strains, the total biomass was significantly lower when in the presence of fungal hyphae (two-sample two-sided Welch test;  $p = 0.0001$ ,  $n = 5$ ) (Figure S5E). Thus, the increased extent of range expansion when in the presence of fungal hyphae was not caused by improved growth of the bacterial strains (e.g., via positive metabolic interactions with the fungus) but was instead likely caused by improved dispersal across the hyphal network.

### Fungal hyphae counteract the loss of spatial intermixing during range expansion in an interaction-independent manner

We next tested whether the effects of fungal hyphae on bacterial diversity during range expansion extend beyond competitive interactions. To test this, we used isogenic mutant strains of *P. stutzeri* A1601 (strains A1602 and A1603) that cross-feed the metabolic intermediate nitrite ( $\text{NO}_2^-$ ) when grown under anoxic

conditions with nitrate ( $\text{NO}_3^-$ ) as the growth-limiting resource (Figures 1A and 3).<sup>50</sup> As we observed for the competing pairs of bacterial strains, the fungal hyphae significantly increased spatial intermixing at the expansion frontier for the cross-feeding pair (two-sample two-sided Welch test;  $p < 7 \times 10^{-6}$ ,  $n = 5$ ) (Figures 3C [local-scale Fourier transform method] and 3D [intersection method]). This effect size is remarkably consistent with that measured for the competing pair of *P. stutzeri* A1601 strains (Figures 2F and 3C), indicating that the effect size is largely interaction independent. Also consistent with the competing pairs of bacterial strains, we found that fungal hyphae increased consortium-level expansion distances (two-sample two-sided Welch test;  $p = 1 \times 10^{-9}$ ,  $n = 5$ ) (Figure S5C) while reducing total biomass (two-sample two-sided Welch test;  $p = 0.003$ ,  $n = 5$ ) (Figure S5F). Thus, the presence of fungal hyphae had positive effects on bacterial diversity and the extent of consortium-level expansion in an interaction-independent manner.

### Flagellum-mediated motility is essential for improved bacterial dispersal in the presence of fungal hyphae

To identify the mechanism of bacterial dispersal along fungal hyphae, we conducted additional range expansion experiments with *P. aeruginosa* PAO1 strains that have a loss-of-function deletion in either the type IV pilus-encoding *pilA* gene (strain PAO1- $\Delta pilA$ -*rfp*) or the flagellum-encoding *fliC* gene (strain PAO1- $\Delta fliC$ -*rfp*). We found that the ancestral PAO1-*rfp* and the PAO1- $\Delta pilA$ -*rfp* strains dispersed along the hyphal network, whereas the PAO1- $\Delta fliC$ -*rfp* strain did not (Figures 4A–4C). The radii of the range expansions formed by the PAO1- $\Delta fliC$ -*rfp* strain were significantly smaller than those formed by the PAO1- $\Delta pilA$ -*rfp* strain (two-sample two-sided Welch test;  $p = 3 \times 10^{-6}$ ,  $n = 3$ ) and the ancestral PAO1-*rfp* strain (two-sample two-sided Welch test;  $p = 4 \times 10^{-7}$ ,  $n = 3$ ) (Figure 4D). The radii of the range expansions formed by the PAO1- $\Delta pilA$ -*rfp* strain were also significantly smaller than those

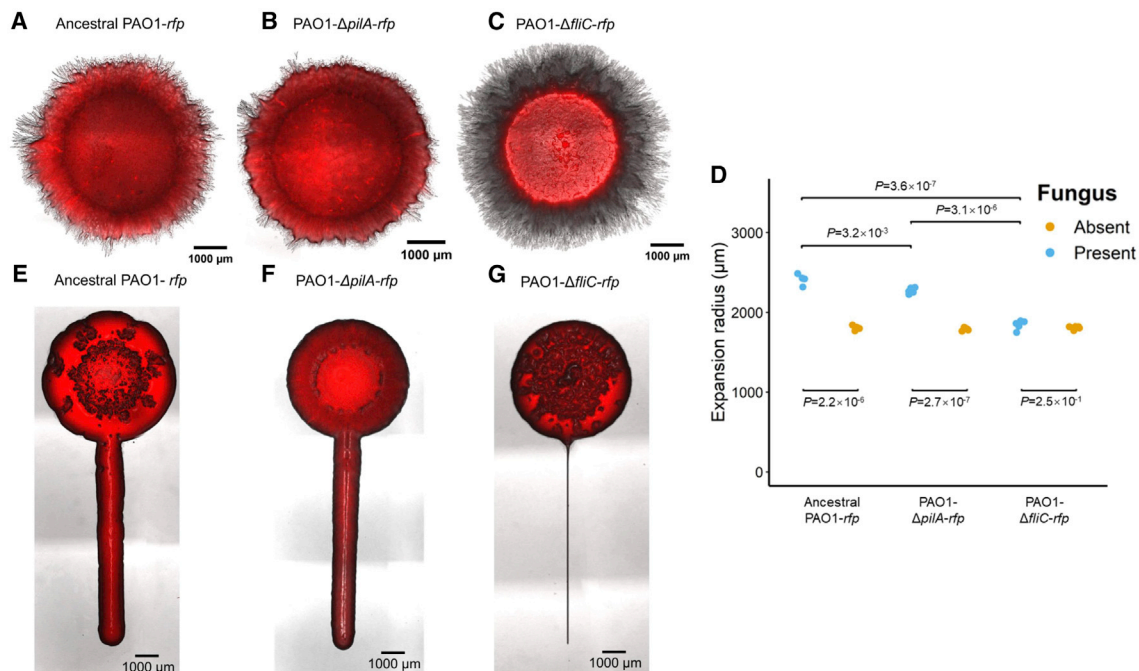


**Figure 4. Effect of defects in pili and flagellum-mediated motility on the extent of range expansion in the presence of fungal hyphae**

(A–C) Representative images of (A) the ancestral *P. aeruginosa* PAO1-*rfp* strain with functional flagella and pili, (B) the PAO1- $\Delta$ *pilA-rfp* strain that is defective in pili-mediated motility, and (C) the PAO1- $\Delta$ *fliC-rfp* strain that is defective in flagellum-mediated motility after 4 days of range expansion. We mixed each bacterial strain individually with *Penicillium* sp. laika and inoculated them onto a separate nutrient-amended agar plate.

(D) Quantification of the total expansion radius for each bacterial strain. Each data point is the measurement for an independent experimental replicate ( $n = 5$ ), and  $p$  is for a two-sample two-sided Welch test with a Holm-Bonferroni correction.

(E–G) We used a glass fiber with a diameter of 5  $\mu$ m as an abiotic surrogate for fungal hyphae. Representative confocal laser scanning microscopy (CLSM) images are for (E) the ancestral *P. aeruginosa* PAO1-*rfp* strain with a functional flagellum and pili, (F) the PAO1- $\Delta$ *pilA-rfp* strain that is defective in pili-mediated motility, and (G) the PAO1- $\Delta$ *fliC-rfp* strain that is defective in flagellum-mediated motility after 4 days of range expansion.

formed by the ancestral PAO1-*rfp* strain (Welch two-sample two-sided t test;  $p = 0.003$ ,  $n = 3$ ), albeit with a smaller effect size (Figure 4D). In contrast, the radii of the range expansions were statistically identical for all the strains in the absence of *Penicillium* sp. laika (Welch two-sample two-sided t test;  $p > 0.5$ ,  $n = 3$ ) (Figure 4D). We performed additional experiments to rule out biological interactions with *Penicillium* sp. laika. Briefly, we allowed the strains to come into contact with a 5  $\mu$ m-diameter glass fiber during range expansion, where the glass fiber promotes the formation of a thin aqueous water film. Consistent with our experiments with fungal hyphae, the ancestral PAO1-*rfp* and the PAO1- $\Delta$ *pilA-rfp* strains dispersed along the glass fiber, whereas the PAO1- $\Delta$ *fliC-rfp* strain did not (Figures 4E–4G). Moreover, when using pairs of competing or cross-feeding bacterial strains, we found that the strains co-migrate along the glass fiber (Figure 5). Thus, a functional flagellum is essential to explain the improved dispersal across fungal hyphae, and the improved dispersal and intermixing are likely consequences of the hydrodynamic environment created by fungal hyphae rather than a consequence of biological interactions with the fungus itself.

#### Topographical effects cannot explain the effects of fungal hyphae on the maintenance of diversity

In addition to increasing the dispersal and expansion range of bacterial individuals, the complex topography of the hyphal

network could also have positive effects on the maintenance of diversity via increased spatial heterogeneity.<sup>51,52</sup> Spaces between the hyphae could spatially segregate distinct bacterial populations and allow their simultaneous occurrence. We tested for this effect by quantifying the degree of spatial intermixing between pairs of *P. aeruginosa* PAO1 strains that are unable to produce a functional flagellum (strains PAO1- $\Delta$ *fliC-rfp* and PAO1- $\Delta$ *fliC-gfp*). In the absence of a functional flagellum, the spatial intermixing of such populations should be solely due to the hyphal network topography and ecological drift. We found that spatial intermixing in the presence or absence of a hyphal network is statistically identical (two-sample two-sided Welch test;  $p = 0.4$ ,  $n = 3$ ) (Figures 6A–6C), indicating a lack of apparent topographical effects. Our scanning electron microscopy images support this finding by showing many instances where bacterial cells migrated over the hyphae and dispersed across the spaces between hyphae (Figure 6D). Thus, topography cannot explain our experimentally observed effects of fungal hyphae on the maintenance of diversity during bacterial range expansion.

#### Fungal hyphae promote conjugation-mediated functional novelty

We finally tested whether the presence of fungal hyphae can promote plasmid conjugation between strains and thus promote the emergence of functional novelty. Our reasoning is that fungal hyphae increase the spatial intermixing of bacterial strains

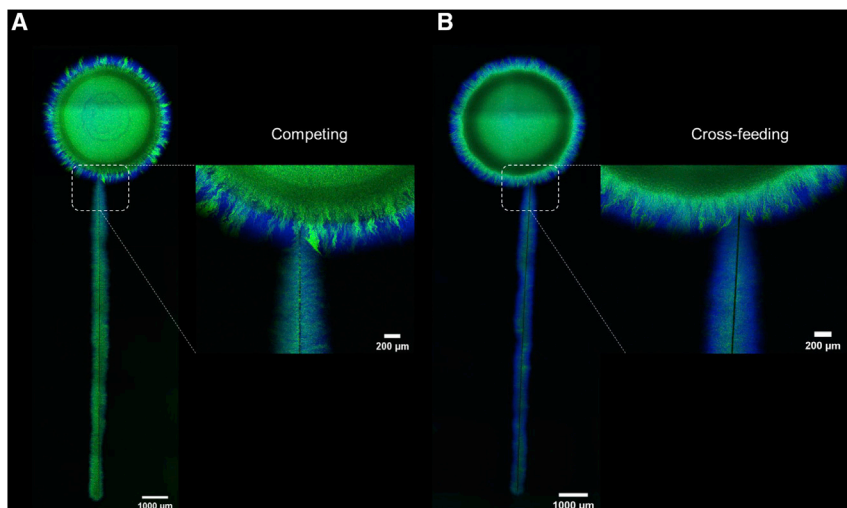


**Figure 5. Range expansions of interacting bacterial strains along a glass fiber**

We used a glass fiber with a diameter of 5  $\mu\text{m}$  as an abiotic surrogate for fungal hyphae, thus allowing us to exclude potential biotic interactions that may affect dispersal abilities and intermixing. Representative confocal laser scanning microscopy images are for (A) the competing pair of *P. stutzeri* A1601 strains and (B) the cross-feeding pair of *P. stutzeri* A1602 and A1603 strains. Note that both strains rapidly co-migrated along the glass fiber, regardless of the interaction imposed between them.

(Figures 2 and 3), which in turn increases the number of interspecific cell-cell contacts and the extent of plasmid conjugation. To test this, we used the competing pair of *P. stutzeri* A1601 strains where one expresses red (*P. stutzeri* A1601-*ech*) and the other expresses green (*P. stutzeri* A1601-*egfp*) fluorescent protein

(Table S1). Both of these fluorescent proteins are encoded by genes introduced into the same neutral site in the chromosome.<sup>15</sup> Both strains also have a loss-of-function mutation in the competence-enabling *comA* gene (Table S1), which prevents transformation of these fluorescent protein-encoding genes between the bacterial strains.<sup>50</sup> We then introduced plasmid pAR145 into *P. stutzeri* A1601-*egfp*, which encodes for chloramphenicol resistance and cyan fluorescent protein (Table S1) and performed range

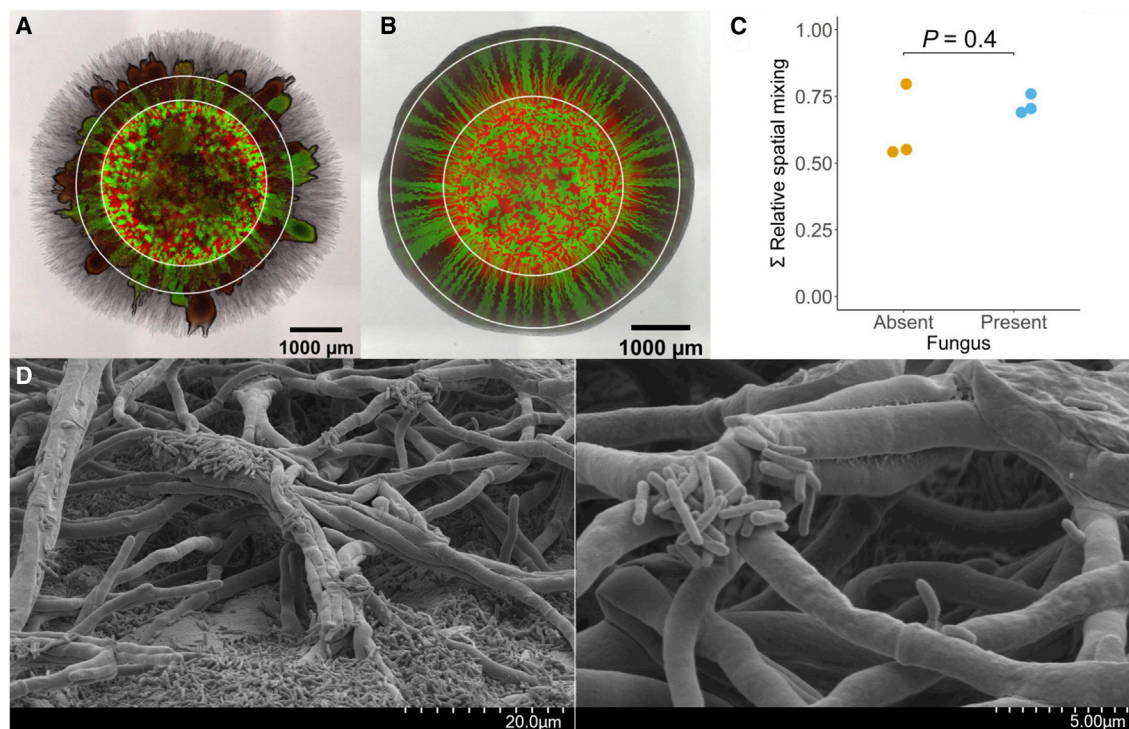


**Figure 6. Range expansions of pairs of *P. aeruginosa* PAO1- $\Delta$ *fliC* strains in the presence or absence of fungal hyphae**

(A and B) Representative images after 4 days of range expansion in the (A) presence or (B) absence of *Penicillium* sp. laika. White circles depict the inoculation area (inner) and a fixed distance within the expansion region where spatial intermixing was clearly affected by fungal hyphae (outer).

(C) We quantified the intermixing index using the local-scale Fourier transform method at radial increments of 5  $\mu\text{m}$  between the outer edge of the inoculation area (inner circle) and the outer edge of the expansion area (outer circle). We corrected each measurement by the circumference at which it was measured and summed all the indices across the expansion area for each replicate. Each data point is a measurement for an independent experimental replicate ( $n = 3$ ), and  $p$  is for a two-sample two-sided Welch test.

(D) Scanning electron microscopy images. Note that the bacteria occupy the surface of the hyphae as well as the interstices between them.

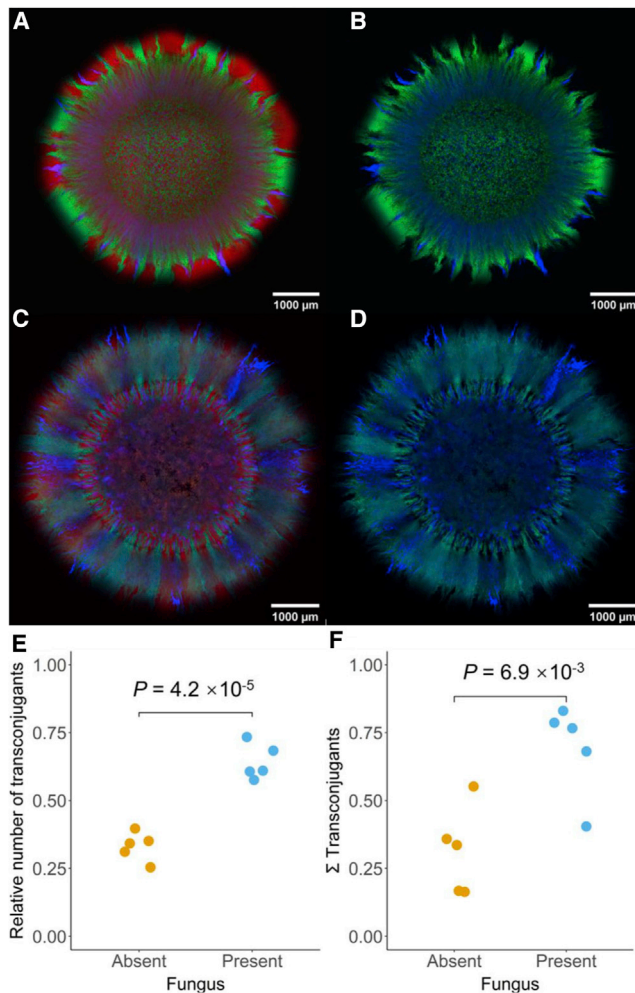


**Figure 7. Plasmid conjugation between competing bacterial strains during range expansion in the absence or presence of fungal hyphae**

(A–D) Representative images of the competing pair of *P. stutzeri* A1601 strains after 4 days of range expansion in the (A and B) absence or (C and D) presence of *Penicillium* sp. laika. In this system, *P. stutzeri* A1601-*egfp* carried plasmid pAR145 and was the plasmid donor strain, whereas *P. stutzeri* A1601-*ech* was the potential recipient strain. pAR145 encodes for chloramphenicol resistance and cyan fluorescent protein. Thus, regions in blue within the expansion area indicate pAR145 presence. (A and C) Composite images of the green, red, and blue channels.

(B and D) Images of only the green and blue channels, which aids in the visualization of transconjugants.

Note that we increased the intensity of the green channel, which caused plasmid donors to appear as only green and improved visual contrast between plasmid donors and transconjugants.

(E) Number of transconjugants relative to the total number of potential recipients across the entire area.

(F) Integrated number of transconjugants relative to the expansion circumference at a given radius over the leading 350  $\mu\text{m}$ -radial region of the expansion area, which corresponds to the expansion region after spatial segregation of the strains in the absence of fungal hyphae. We chose this distance because it corresponds to the area where the hyphal network clearly influences spatial intermixing via bacterial dispersal.

For (E) and (F), each data point is the measurement for an independent experimental replicate ( $n = 5$ ), and  $p$  is for a two-sample two-sided Welch test.

expansions in the absence of chloramphenicol (i.e., we did not impose selection for transconjugants). Areas within the expansion region where both red and cyan (but not green) fluorescent proteins are expressed indicate regions where pAR145 successfully conjugated into *P. stutzeri* A1601-*ech*.

Using the same experimental design as for our other range expansion experiments, we observed conjugation of pAR145 to *P. stutzeri* A1601-*ech* both in the absence (Figures 7A and 7B) and presence (Figures 7C and 7D) of fungal hyphae. These events are identifiable as blue patches within the expansion area. As expected, fungal hyphae increased the extent of plasmid conjugation both within the entire area (two-sample two-sided Welch test;  $p = 4 \times 10^{-5}$ ,  $n = 5$ ) (Figure 7E) and within only the expansion area (two-sample two-sided Welch test;  $p = 0.007$ ,  $n = 5$ ) (Figure 7F). Thus, the presence of fungal hyphae not only counteracts the loss of diversity during bacterial range expansion but also promotes the emergence of plasmid-mediated functional novelty.

## DISCUSSION

Our study revealed that hyphal networks can regulate bacterial diversity during range expansion. Ecological drift at the expansion frontier and resource limitations behind the expansion frontier have strong purging effects on the diversity of surface-associated microbial communities,<sup>7,8,19,53</sup> which is apparent in the highly segregated spatial patterns that characterize competition-dominated systems.<sup>9</sup> The hyphal network increases spatial intermixing by increasing the dispersal capabilities of individuals that would otherwise only disperse via cell-shoving and short-range twitching. These factors promote the simultaneous proliferation of larger numbers of spatially segregated bacterial populations, reflecting the maintenance of diversity during range expansion (Figures 2 and 3). Our results therefore provide evidence that frequent long-distance dispersal can increase expansion speeds and promote the maintenance of microbial diversity over time.<sup>49,54–56</sup>

In our system, bacterial dispersal along fungal hyphae is driven by active flagellar motility that enables individuals to colonize unoccupied space (Figures 4 and 5), which accelerates range expansion and alleviates the effects of ecological drift. We found that the mechanism mediating this process is the micro-hydro-physical environment created by fungal hyphae, which we demonstrated using a glass fiber as a simple physical surrogate of fungal hyphal structure that allowed us to exclude specific biological interactions and processes (e.g., chemotaxis<sup>57</sup> or secretion of signal inducing molecules<sup>31</sup>) (Figures 4 and 5). Under the physical conditions created by the glass fiber, we observed co-migration and increased intermixing of bacterial strains, regardless of the interactions that occurred between them (Figure 5). This means that as long as fungal hyphae and their associated thin water films are present (which may vary with hydration conditions), local bacterial diversity and intermixing can be maintained regardless of whether the fungus is physiologically active or not.

In a system where the probability of dispersal upon contact with a fungal hypha is low and the available nutrients are not sufficient to support rapid proliferation, the presence of fungal hyphae will also create a heterogeneous topography that could

spatially isolate different populations and increase microbial diversity globally.<sup>58</sup> For example, recent research demonstrated that differential dispersal across hyphal networks by bacteria with different motility strategies determined the diversity and composition of cheese rind microbiomes.<sup>36</sup> Besides trait differences between taxa, the maintenance of bacterial diversity across surfaces with heterogeneous topographies such as soils or activated sludge can be controlled by host-mediated dispersal (e.g., invertebrates),<sup>59,60</sup> by the transient changes to hydration conditions,<sup>61</sup> or by the pore structure of the matrix where range expansion occurs.<sup>25</sup> These factors can rescue microbial populations undergoing extinction due to ecological drift by promoting spatial isolation. Our study demonstrates that hyphal networks and their associated thin water films alone can promote the maintenance of microbial diversity during range expansion without the need for such topographical effects (Figure 6). Future work could improve the transfer of our findings to natural systems by adding additional processes to the experimental system such as periodic evaporation/hydration or the addition of burrowing eukaryotes and then quantify the strength of the fungal hyphae-mediated effects on counteracting drift in the presence or absence of these additional processes.

We finally found that bacterial communities that expand in the presence of hyphal networks have an increased extent of plasmid conjugation between local populations during range expansion (Figure 7). A previous study demonstrated that fungal hyphae enable the long-range movement of plasmid donors and potential recipients that are otherwise spatially isolated in separate colonies.<sup>41</sup> This increases the number of interspecific cell-cell contacts and promotes plasmid conjugation.<sup>41</sup> Hydration dynamics in unsaturated environments can also enable the long-range movement of plasmid donors and potential recipients, increase the number of interspecific cell-cell contacts, and promote plasmid conjugation.<sup>62,63</sup> In soils, even earthworms can enable such long-range movements and increase horizontal gene transfer at the level of the entire soil matrix.<sup>64</sup> Our findings provide additional insights into fungal hyphae-mediated dispersal by demonstrating that they cause higher spatial intermixing of plasmid donors and potential recipients at local scales within a single colony, which in turn also promotes plasmid conjugation. Thus, fungal hyphae can promote the spread of plasmid-encoded traits over a range of length scales, from local scales within individual expanding colonies to longer scales between colonies. Such conclusions are not limited to antibiotic resistance-encoding plasmids but could be of relevance to a variety of plasmids, including those important for virulence, environmental remediation, and biotechnology.

## STAR★METHODS

Detailed methods are provided in the online version of this paper and include the following:

- KEY RESOURCES TABLE
- RESOURCE AVAILABILITY
  - Lead contact
  - Materials availability
  - Data and code availability

## ● EXPERIMENTAL MODEL AND SUBJECT DETAILS

- Microbial strains

## ● METHOD DETAILS

- Experimental procedure to test the effects of fungal hyphae on bacterial range expansion
- Experimental procedure used to test the effects of active motility on bacterial range expansion
- Experimental procedure used to test for possible topographical effects caused by the fungal hyphae
- Experimental procedure used to test the effects of fungal hyphae on plasmid conjugation
- Confocal laser scanning microscopy
- Scanning electron microscopy (SEM)

## ● QUANTIFICATION AND STATISTICAL ANALYSIS

- Quantification of spatial intermixing
- Quantification of plasmid pAR145ecfp transconjugants during range expansion
- Quantification of biomass
- Statistical analyses

## SUPPLEMENTAL INFORMATION

Supplemental information can be found online at <https://doi.org/10.1016/j.cub.2022.11.009>.

## ACKNOWLEDGMENTS

C.R. was supported by grants from the National Natural Science Foundation of China (42277298) and the 2115 Talent Development Program of the China Agricultural University (1191-00109012) awarded to G.W. C.R. was also supported by a grant from China Scholarship Council, State Scholarship fund. J.R. was supported by a grant from the Swiss National Science Foundation (P2EZP3\_199849) awarded to J.R. and an Eawag Discretionary Funds grant (category SEED) awarded to D.R.J. G.G. was supported by a grant from the Swiss National Science Foundation (310030\_188642) awarded to Martin Ackermann. We thank Professor Liqun Zhang, Department of Plant Pathology, China Agricultural University, for providing the *Pseudomonas aeruginosa* PAO1 strains and Dr. Maria Pilar Garcillán-Barcia, Instituto de Biomedicina y Biología, University of Cantabria, for providing plasmid pAR145ecfp. We thank Dr. Anne Greet Bittermann, Scientific Center for Optical and Electron Microscopy (ETH Zürich, Switzerland) (<https://scopem.ethz.ch/>) for assistance with the scanning electron microscopy. We thank Miaoxiao Wang, Yinyin Ma, and Deepthi Vinod for helpful discussions. Finally, we thank Laika, a 4-year-old Galgo Español (*Canis familiaris*), for graciously allowing us to isolate *Penicillium* sp. laika from her paw.

## AUTHOR CONTRIBUTIONS

C.R. and J.R. contributed equally to this work. C.R., J.R., G.W., and D.R.J. conceived and developed the research question. C.R., J.R., and D.R.J. designed the experiments. C.R. performed the experiments. G.G. developed the intermixing index calculation based on Fourier transforms. C.R., J.R., and G.G. analyzed the data. J.R. and D.R.J. prepared the manuscript. All authors contributed to the interpretation of the results and gave critical input to the final version of the manuscript. D.R.J. and G.W. coordinated the study.

## DECLARATION OF INTERESTS

The authors declare no competing interests.

## INCLUSION AND DIVERSITY

We support inclusive, diverse, and equitable conduct of research.

Received: May 31, 2022  
 Revised: September 20, 2022  
 Accepted: November 3, 2022  
 Published: November 30, 2022

### REFERENCES

- Hall-Stoodley, L., Costerton, J.W., and Stoodley, P. (2004). Bacterial biofilms: from the natural environment to infectious diseases. *Nat. Rev. Microbiol.* **2**, 95–108.
- Flemming, H.C., Wingender, J., Szewzyk, U., Steinberg, P., Rice, S.A., and Kjelleberg, S. (2016). Biofilms: an emergent form of bacterial life. *Nat. Rev. Microbiol.* **14**, 563–575.
- Man, W.H., de Steenhuijsen Piters, W.A.A., and Bogaert, D. (2017). The microbiota of the respiratory tract: gatekeeper to respiratory health. *Nat. Rev. Microbiol.* **15**, 259–270.
- Tilman, D., and Kareiva, P.M. (1997). *Spatial Ecology: The Role of Space in Population Dynamics and Interspecific Interactions* (Princeton University Press), p. MPB-30.
- Excoffier, L., Foll, M., and Petit, R.J. (2009). Genetic consequences of range expansions. *Annu. Rev. Ecol. Evol. Syst.* **40**, 481–501.
- Golding, I., Cohen, I., and Ben-Jacob, E. (1999). Studies of sector formation in expanding bacterial colonies. *Europhys. Lett.* **48**, 587–593.
- Hallatschek, O., Hersen, P., Ramanathan, S., and Nelson, D.R. (2007). Genetic drift at expanding frontiers promotes gene segregation. *Proc. Natl. Acad. Sci. USA* **104**, 19926–19930.
- Hallatschek, O., and Nelson, D.R. (2010). Life at the front of an expanding population. *Evolution* **64**, 193–206.
- Korolev, K.S., Müller, M.J.I., Karahan, N., Murray, A.W., Hallatschek, O., and Nelson, D.R. (2012). Selective sweeps in growing microbial colonies. *Phys. Biol.* **9**, 026008.
- Eckburg, P.B., Bik, E.M., Bernstein, C.N., Purdom, E., Dethlefsen, L., Sargent, M., Gill, S.R., Nelson, K.E., and Relman, D.A. (2005). Diversity of the human intestinal microbial flora. *Science* **308**, 1635–1638.
- Gans, J., Wolinsky, M., and Dunbar, J. (2005). Computational improvements reveal great bacterial diversity and high metal toxicity in soil. *Science* **309**, 1387–1390.
- Human Microbiome Project Consortium (2012). Structure, function and diversity of the healthy human microbiome. *Nature* **486**, 207–214.
- Momeni, B., Brileya, K.A., Fields, M.W., and Shou, W.Y. (2013). Strong inter-population cooperation leads to partner intermixing in microbial communities. *eLife* **2**, e00230.
- Müller, M.J.I., Neugeboren, B.I., Nelson, D.R., and Murray, A.W. (2014). Genetic drift opposes mutualism during spatial population expansion. *Proc. Natl. Acad. Sci. USA* **111**, 1037–1042.
- Goldschmidt, F., Regoes, R.R., and Johnson, D.R. (2017). Successive range expansion promotes diversity and accelerates evolution in spatially structured microbial populations. *ISME J.* **11**, 2112–2123.
- Hibbing, M.E., Fuqua, C., Parsek, M.R., and Peterson, S.B. (2010). Bacterial competition: surviving and thriving in the microbial jungle. *Nat. Rev. Microbiol.* **8**, 15–25.
- Foster, K.R., and Bell, T. (2012). Competition, not cooperation, dominates interactions among culturable microbial species. *Curr. Biol.* **22**, 1845–1850.
- Palmer, J.D., and Foster, K.R. (2022). Bacterial species rarely work together. *Science* **376**, 581–582.
- Mitri, S., Clarke, E., and Foster, K.R. (2016). Resource limitation drives spatial organization in microbial groups. *ISME J.* **10**, 1471–1482.
- Goldschmidt, F., Regoes, R.R., and Johnson, D.R. (2018). Metabolite toxicity slows local diversity loss during expansion of a microbial cross-feeding community. *ISME J.* **12**, 136–144.
- van Gestel, J., Weissing, F.J., Kuipers, O.P., and Kovács, A.T. (2014). Density of founder cells affects spatial pattern formation and cooperation in *Bacillus subtilis* biofilms. *ISME J.* **8**, 2069–2079.
- Goldschmidt, F., Caduff, L., and Johnson, D.R. (2021). Causes and consequences of pattern diversification in a spatially self-organizing microbial community. *ISME J.* **15**, 2415–2426.
- Eigentler, L., Kalamara, M., Ball, G., MacPhee, C.E., Stanley-Wall, N.R., and Davidson, F.A. (2022). Founder cell configuration drives competitive outcome within colony biofilms. *ISME J.* **16**, 1512–1522.
- Ciccarese, D., Zuidema, A., Merlo, V., and Johnson, D.R. (2020). Interaction-dependent effects of surface structure on microbial spatial self-organization. *Philos. Trans. R. Soc. Lond. B Biol. Sci.* **375**, 20190246.
- Carson, J.K., Gonzalez-Quiriones, V., Murphy, D.V., Hinz, C., Shaw, J.A., and Gleeson, D.B. (2010). Low pore connectivity increases bacterial diversity in soil. *Appl. Environ. Microbiol.* **76**, 3936–3942.
- de Boer, Wd, Folman, L.B., Summerbell, R.C., and Boddy, L. (2005). Living in a fungal world: impact of fungi on soil bacterial niche development. *FEMS Microbiol. Rev.* **29**, 795–811.
- Hogan, D.A., and Kolter, R. (2002). *Pseudomonas-Candida* interactions: an ecological role for virulence factors. *Science* **296**, 2229–2232.
- Underhill, D.M., and Iliev, I.D. (2014). The mycobiota: interactions between commensal fungi and the host immune system. *Nat. Rev. Immunol.* **14**, 405–416.
- van Overbeek, L.S., and Saikkonen, K. (2016). Impact of bacterial-fungal interactions on the colonization of the endosphere. *Trends Plant Sci.* **21**, 230–242.
- Tipton, L., Müller, C.L., Kurtz, Z.D., Huang, L., Kleerup, E., Morris, A., Bonneau, R., and Ghedin, E. (2018). Fungi stabilize connectivity in the lung and skin microbial ecosystems. *Microbiome* **6**, 12.
- Frey-Klett, P., Burlinson, P., Deveau, A., Barret, M., Tarkka, M., and Sarniguet, A. (2011). Bacterial-fungal interactions: hyphens between agricultural, clinical, environmental, and food microbiologists. *Microbiol. Mol. Biol. Rev.* **75**, 583–609.
- Kohlmeier, S., Smits, T.H.M., Ford, R.M., Keel, C., Harms, H., and Wick, L.Y. (2005). Taking the fungal highway: mobilization of pollutant-degrading bacteria by fungi. *Environ. Sci. Technol.* **39**, 4640–4646.
- Warmink, J.A., Nazir, R., Corten, B., and van Elsas, J.D. (2011). Hitchhikers on the fungal highway: the helper effect for bacterial migration via fungal hyphae. *Soil Biol. Biochem.* **43**, 760–765.
- Pion, M., Bshary, R., Bindschedler, S., Filippidou, S., Wick, L.Y., Job, D., and Junier, P. (2013). Gains of bacterial flagellar motility in a fungal world. *Appl. Environ. Microbiol.* **79**, 6862–6867.
- Worrhick, A., König, S., Miltner, A., Banitz, T., Centler, F., Frank, K., Thullner, M., Harms, H., Kästner, M., and Wick, L.Y. (2016). Mycelium-like networks increase bacterial dispersal, growth, and biodegradation in a model ecosystem at various water potentials. *Appl. Environ. Microbiol.* **82**, 2902–2908.
- Zhang, Y.C., Kastman, E.K., Guasto, J.S., and Wolfe, B.E. (2018). Fungal networks shape dynamics of bacterial dispersal and community assembly in cheese rind microbiomes. *Nat. Commun.* **9**, 336.
- Xiong, B.J., Kleinstuber, S., Sträuber, H., Dusny, C., Harms, H., and Wick, L.Y. (2022). Impact of fungal hyphae on growth and dispersal of obligate anaerobic bacteria in aerated habitats. *mBio* **13**, e0076922.
- Wick, L.Y., Remer, R., Würz, B., Reichenbach, J., Braun, S., Schäfer, F., and Harms, H. (2007). Effect of fungal hyphae on the access of bacteria to phenanthrene in soil. *Environ. Sci. Technol.* **41**, 500–505.
- Furuno, S., Pätzold, K., Rabe, C., Neu, T.R., Harms, H., and Wick, L.Y. (2009). Fungal mycelia allow chemotactic dispersal of polycyclic aromatic hydrocarbon-degrading bacteria in water-unsaturated systems. *Environ. Microbiol.* **12**, 1391–1398.
- Banitz, T., Fetzter, I., Johst, K., Wick, L.Y., Harms, H., and Frank, K. (2011). Assessing biodegradation benefits from dispersal networks. *Ecol. Modell.* **222**, 2552–2560.
- Berthold, T., Centler, F., Hübschmann, T., Remer, R., Thullner, M., Harms, H., and Wick, L.Y. (2016). Mycelia as a focal point for horizontal gene transfer among soil bacteria. *Sci. Rep.* **6**, 36390.

42. Otto, S., Bruni, E.P., Harms, H., and Wick, L.Y. (2017). Catch me if you can: dispersal and foraging of *Bdellovibrio bacteriovorus* 109J along mycelia. *ISME J.* *11*, 386–393.
43. You, X., Kallies, R., Kühn, I., Schmidt, M., Harms, H., Chatzinotas, A., and Wick, L.Y. (2022). Phage co-transport with hyphal-riding bacterial fuels bacterial invasion in a water-unsaturated microbial model system. *ISME J.* *16*, 1275–1283.
44. Tilman, D. (1994). Competition and biodiversity in spatially structured habitats. *Ecol.* *75*, 2–16.
45. Nadell, C.D., and Bassler, B.L. (2011). A fitness trade-off between local competition and dispersal in *Vibrio cholerae* biofilms. *Proc. Natl. Acad. Sci. USA* *108*, 14181–14185.
46. Datta, M.S., Korolev, K.S., Cvijovic, I., Dudley, C., and Gore, J. (2013). Range expansion promotes cooperation in an experimental microbial metapopulation. *Proc. Natl. Acad. Sci. USA* *110*, 7354–7359.
47. Yawata, Y., Cordero, O.X., Menolascina, F., Hehemann, J.H., Polz, M.F., and Stocker, R. (2014). Competition-dispersal tradeoff ecologically differentiates recently speciated marine bacterioplankton populations. *Proc. Natl. Acad. Sci. USA* *111*, 5622–5627.
48. Gude, S., Pinçe, E., Taute, K.M., Seinen, A.B., Shimizu, T.S., and Tans, S.J. (2020). Bacterial coexistence driven by motility and spatial competition. *Nature* *578*, 588–592.
49. Paulose, J., and Hallatschek, O. (2020). The impact of long-range dispersal on gene surfing. *Proc. Natl. Acad. Sci. USA* *117*, 7584–7593.
50. Lilja, E.E., and Johnson, D.R. (2016). Segregating metabolic processes into different microbial cells accelerates the consumption of inhibitory substrates. *ISME J.* *10*, 1568–1578.
51. Silvertown, J., Dodd, M.E., Gowing, D.J.G., and Mountford, J.O. (1999). Hydrologically defined niches reveal a basis for species richness in plant communities. *Nature* *400*, 61–63.
52. Hart, S.P., Usinowicz, J., and Levine, J.M. (2017). The spatial scales of species coexistence. *Nat. Ecol. Evol.* *1*, 1066–1073.
53. Weinstein, B.T., Lavrentovich, M.O., Möbius, W., Murray, A.W., and Nelson, D.R. (2017). Genetic drift and selection in many-allele range expansions. *PLoS Comput. Biol.* *13*, e1005866.
54. Davies, S., White, A., and Lowe, A. (2004). An investigation into effects of long-distance seed dispersal on organelle population genetic structure and colonization rate: a model analysis. *Heredity* *93*, 566–576.
55. Bialozyt, R., Ziegenhagen, B., and Petit, R.J. (2006). Contrasting effects of long distance seed dispersal on genetic diversity during range expansion. *J. Evol. Biol.* *19*, 12–20.
56. Fayard, J., Klein, E.K., and Lefèvre, F. (2009). Long distance dispersal and the fate of a gene from the colonization front. *J. Evol. Biol.* *22*, 2171–2182.
57. Haq, I.U., Calixto, R.O.D., Yang, P., dos Santos, G.M.P., Barreto-Bergter, E., and van Elsas, J.D. (2016). Chemotaxis and adherence to fungal surfaces are key components of the behavioral response of *Burkholderia terrae* BS001 to two selected soil fungi. *FEMS Microbiol. Ecol.* *92*, fiw164.
58. Chesson, P. (2000). General theory of competitive coexistence in spatially-varying environments. *Theor. Popul. Biol.* *58*, 211–237.
59. Domínguez, J., Aira, M., Crandall, K.A., and Pérez-Losada, M. (2021). Earthworms drastically change fungal and bacterial communities during vermicomposting of sewage sludge. *Sci. Rep.* *11*, 15556.
60. Ruddick, S.M., and Williams, S.T. (1972). Studies on the ecology of actinomycetes in soil V. Some factors influencing the dispersal and adsorption of spores in soil. *Soil Biol. Biochem.* *4*, 93–103.
61. Trevors, J.T., van Elsas, J.D., van Overbeek, L.S., and Starodub, M.E. (1990). Transport of genetically engineered *Pseudomonas fluorescens* strain through a soil microcosm. *Appl. Environ. Microbiol.* *56*, 401–408.
62. Tecon, R., Ebrahimi, A., Kleyer, H., Erev Levi, S.E., and Or, D. (2018). Cell-to-cell bacterial interactions promoted by drier conditions on soil surfaces. *Proc. Natl. Acad. Sci. USA* *115*, 9791–9796.
63. Ruan, C., Ramoneda, J., Chen, G., Johnson, D.R., and Wang, G. (2021). Evaporation-induced hydrodynamics promote conjugation-mediated plasmid transfer in microbial populations. *ISME COMMUN.* *1*, 54.
64. Daane, L.L., Molina, J.A., Berry, E.C., and Sadowsky, M.J. (1996). Influence of earthworm activity on gene transfer from *Pseudomonas fluorescens* to indigenous soil bacteria. *Appl. Environ. Microbiol.* *62*, 515–521.
65. Lilja, E.E., and Johnson, D.R. (2019). Substrate cross-feeding affects the speed and trajectory of molecular evolution within a synthetic microbial assemblage. *BMC Evol. Biol.* *19*, 129.
66. Wang, S., Yu, S., Zhang, Z., Wei, Q., Yan, L., Ai, G., Liu, H., and Ma, L.Z. (2014). Coordination of swarming motility, biosurfactant synthesis, and biofilm matrix exopolysaccharide production in *Pseudomonas aeruginosa*. *Appl. Environ. Microbiol.* *80*, 6724–6732.
67. Wang, S.W., Parsek, M.R., Wozniak, D.J., and Ma, L.Z. (2013). A spider web strategy of type IV pili-mediated migration to build a fibre-like Psl polysaccharide matrix in *Pseudomonas aeruginosa* biofilms. *Environ. Microbiol.* *15*, 2238–2253.
68. Nilsson, R.H., Taylor, A.F.S., Adams, R.I., Baschien, C., Johan Bengtsson-Palme, Cangren, P., Coleine, C., Heide-Marie Daniel, Glassman, S.I., Hirooka, Y., et al. (2018). Taxonomic annotation of public fungal ITS sequences from the built environment - a report from an April 10–11, 2017 workshop (Aberdeen, UK). *MycKeys* *2018*, 65–82.
69. R Core Team (2016). R: A Language and Environment for Statistical Computing (R Foundation for Statistical Computing).
70. Meier, P., Berndt, C., Weger, N., and Wackernagel, W. (2002). Natural transformation of *Pseudomonas stutzeri* by single-stranded DNA requires type IV pili, competence state and *comA*. *FEMS Microbiol. Lett.* *207*, 75–80.
71. Gardes, M., and Bruns, T.D. (1993). ITS primers with enhanced specificity for basidiomycetes - application to the identification of mycorrhizae and rusts. *Mol. Ecol.* *2*, 113–118.
72. Ciccarese, D., Micali, G., Borer, B., Ruan, C., Or, D., and Johnson, D.R. (2022). Rare and localized events stabilize microbial community composition and patterns of spatial self-organization in a fluctuating environment. *ISME J.* *16*, 1453–1463.
73. Prest, E.I., Hammes, F., Kötzsch, S., van Loosdrecht, M.C.M., and Vrouwenvelder, J.S. (2013). Monitoring microbiological changes in drinking water systems using a fast and reproducible flow cytometric method. *Water Res.* *47*, 7131–7142.

## STAR★METHODS

### KEY RESOURCES TABLE

REAGENT or RESOURCE	SOURCE	IDENTIFIER
<b>Chemicals, peptides, and recombinant proteins</b>		
Sodium nitrate	Sigma-Aldrich	S5506
Isopropyl β-D-1-thiogalactopyranoside	Sigma-Aldrich	I6758
Lysogeny broth	Sigma-Aldrich	L1900
Lysogeny broth agar	Sigma-Aldrich	L2025
Kanamycin disulfate	Sigma-Aldrich	K1876
<b>Deposited data</b>		
Original code	ERIC open	<a href="https://doi.org/10.25678/0007GJ">https://doi.org/10.25678/0007GJ</a>
Experimental data	ERIC open	<a href="https://doi.org/10.25678/0007GJ">https://doi.org/10.25678/0007GJ</a>
Sequence data	Genbank	MG818940.1, KT270333.1, KM396384.1, KM396380.1
<b>Experimental models: Organisms/strains</b>		
<i>P. stutzeri</i> A1601- <i>egfp</i>	Lilja and Johnson <sup>50,65</sup>	N/A
<i>P. stutzeri</i> A1601- <i>ech</i>	Lilja and Johnson <sup>50,65</sup>	N/A
<i>P. stutzeri</i> A1601- <i>ecfp</i>	Lilja and Johnson <sup>50,65</sup>	N/A
<i>P. stutzeri</i> A1602- <i>egfp</i>	Lilja and Johnson <sup>50,65</sup>	N/A
<i>P. stutzeri</i> A1603- <i>ecfp</i>	Lilja and Johnson <sup>50,65</sup>	N/A
<i>P. aeruginosa</i> PAO1- <i>gfp</i>	Wang et al. <sup>66</sup>	N/A
<i>P. aeruginosa</i> PAO1- <i>rfp</i>	Wang et al. <sup>67</sup>	N/A
<i>P. aeruginosa</i> PAO1-Δ <i>flhC</i> - <i>rfp</i>	Wang et al. <sup>66,67</sup>	N/A
<i>P. aeruginosa</i> PAO1-Δ <i>flhC</i> - <i>gfp</i>	Wang et al. <sup>66,67</sup>	N/A
<i>P. aeruginosa</i> PAO1-Δ <i>pilA</i> - <i>rfp</i>	Wang et al. <sup>66,67</sup>	N/A
<i>Penicillium</i> sp. laika	This study	N/A
<b>Software and algorithms</b>		
UNITE	Nilsson et al. <sup>68</sup>	<a href="https://unite.ut.ee/">https://unite.ut.ee/</a>
BLAST	NCBI	<a href="https://blast.ncbi.nlm.nih.gov/Blast.cgi">https://blast.ncbi.nlm.nih.gov/Blast.cgi</a>
Fiji (v1.53C)	Fiji	<a href="https://fiji.sc">https://fiji.sc</a>
ImageJ	ImageJ	<a href="https://imagej.net">https://imagej.net</a>
R/RStudio	R Core Team <sup>69</sup>	<a href="http://www.Rproject.org/">http://www.Rproject.org/</a>

### RESOURCE AVAILABILITY

#### Lead contact

Further information and requests for resources, reagents and microbial strains should be directed to and will be fulfilled by the lead contact David R. Johnson ([david.johnson@eawag.ch](mailto:david.johnson@eawag.ch)).

#### Materials availability

All fungal and bacterial strains generated in this study are available from the lead contact with a completed Materials Transfer Agreement.

#### Data and code availability

All data and code have been deposited in the Eawag Research Data Institutional Repository (<https://opendata.eawag.ch/>) and are publicly available as of the date of publication at the following DOI: (<https://doi.org/10.25678/0007GJ>).

## EXPERIMENTAL MODEL AND SUBJECT DETAILS

## Microbial strains

We used isogenic mutants of *P. stutzeri* A1601<sup>15,50</sup> and *P. aeruginosa* PAO1 to test the effects of fungal hyphae on the maintenance of bacterial diversity during range expansion. We assembled these strains into three pairs. The first pair consisted of *P. stutzeri* A1601-*egfp* and A1601-*ecfp* (Figure 1A; Table S1). Both of these strains have the complete denitrification pathway and, aside from having different chromosomally located fluorescent protein-encoding genes, are genetically identical.<sup>15,50</sup> They thus compete with each other when grown together in an anoxic environment with nitrate (NO<sub>3</sub><sup>-</sup>) as the growth-limiting resource. The second pair consisted of *P. stutzeri* A1602-*egfp* and A1603-*ecfp* (Figure 1A; Table S1). Strain A1602-*egfp* has a loss-of-function deletion in the nitrate reductase-encoding *narG* gene while strain A1603-*ecfp* has a loss-of-function deletion in the nitrite (NO<sub>2</sub><sup>-</sup>) reductase-encoding *nirS* gene.<sup>50</sup> They therefore engage in a nitrite cross-feeding interaction when grown together in an anoxic environment with nitrate as the growth-limiting nutrient.<sup>50</sup> All the *P. stutzeri* strains also have a loss-of-function deletion in the *comA* gene that prevents recombination when grown together<sup>50,70</sup> and a chromosomally located gentamycin resistance gene to prevent contamination during experiments.<sup>65</sup> All the *P. stutzeri* strains have a chromosomally located isopropyl β-D-1-thiogalactopyranoside (IPTG)-inducible fluorescent protein-encoding gene that encodes for either cyan or green fluorescent protein,<sup>15,65</sup> which enables us to distinguish them by fluorescence microscopy when grown together. A complete description of the strains, along with details of their genetic construction, are reported in detail elsewhere.<sup>15,50,65</sup> The third pair consisted of *P. aeruginosa* PAO1-*gfp* and PAO1-*rfp* (Figure 1A; Table S1). Strain PAO1-*gfp* carries plasmid pSMC21 that contains the green fluorescent protein-encoding *gfp* gene while strain PAO1-*rfp* carries plasmid pBRM that contains the red fluorescent protein-encoding *rfp* gene (Table S1). As with the *P. stutzeri* A1601 strains, both *P. aeruginosa* PAO1 strains have the complete denitrification pathway and, aside from carrying different plasmid-located fluorescent protein-encoding genes, are genetically identical. They therefore also compete with each other when grown together in an anoxic environment amended with nitrate as the growth-limiting resource. We routinely grew all the *P. stutzeri* and *P. aeruginosa* strains with lysogeny broth (LB) medium at 30°C.

We used the hyphae-forming fungus *Penicillium* sp. laika to test the effects of fungal hyphae on the maintenance of bacterial diversity during range expansion. We isolated this strain from the paw of a Galgo Español (*Canis familiaris*) by physical contact with an LB agar plate supplemented with 50 μg ml<sup>-1</sup> kanamycin. After incubation of the LB agar plate for three days at 20°C, we obtained a white villiform fungal colony and purified the colony by streaking a second time on an LB agar plate supplemented with 50 μg ml<sup>-1</sup> kanamycin. We routinely grew *Penicillium* sp. laika in liquid LB medium at 20°C. We determined the taxonomic affiliation of *Penicillium* sp. laika by Sanger sequencing of a PCR-amplified 520 bp fragment of the internal transcribed spacer region (primers: ITS1 5'-TCCGTAGGTGA ACCTGCGG-3'; ITS4 5'-TCCTCCGCTTATTGATATGC-3').<sup>71</sup> We submitted the consensus sequence to the UNITE database<sup>68</sup> and queried for similar sequences using the BLAST algorithm (<https://blast.ncbi.nlm.nih.gov/Blast.cgi>). The alignment has 100% sequence coverage and 100% sequence identity to GenBank accessions MG818940.1, KT270333.1, KM396384.1, and KM396380.1 assigned to the *Penicillium glabrum/thomii* group. We summarized the morphological characteristics of *Penicillium* sp. laika in Table S1.

## METHOD DETAILS

## Experimental procedure to test the effects of fungal hyphae on bacterial range expansion

To prepare *Penicillium* sp. laika for experimentation, we first grew the strain on oxalic LB agar plates for five days to allow for spore maturation. We then removed the fungal spores from the plate using a sterile inoculation loop and transferred the spores to 1 mL of oxalic 0.9% (w/v) sodium chloride solution. We suspended the spores by vortexing for 10 minutes and adjusted the optical density at 600 nm (OD<sub>600</sub>) to 1. To prepare the bacterial strains for experimentation, we first grew each strain separately overnight in oxalic LB medium at 37°C. After reaching stationary phase, we adjusted the densities of each culture to an OD<sub>600</sub> of 2, centrifuged the cultures at 3600 × g for 5 min at room temperature, discarded the supernatants, and suspended the cells in 1 mL of oxalic 0.9% (w/v) sodium chloride solution. We then mixed the corresponding bacterial strains together at equal initial proportions and diluted the bacterial mixtures to approximately 10<sup>6</sup> colony forming units ml<sup>-1</sup> in 0.9% (w/v) sodium chloride solution.

We performed range expansion experiments using a modified version of a protocol described in detail elsewhere.<sup>15,20</sup> Briefly, for experiments with pairs of *P. stutzeri* or *P. aeruginosa* strains, we mixed equal volumes of the fungal and bacterial solutions and deposited a single 2 μl droplet onto the middle of a modified oxalic LB agar plate. The modified LB agar plate contained 10 g L<sup>-1</sup> tryptone, 5 g L<sup>-1</sup> yeast extract, 10 g L<sup>-1</sup> sodium chloride, 20 g L<sup>-1</sup> agar, 20 mM sodium nitrate (NO<sub>3</sub><sup>-</sup>), and 100 μM IPTG. We then incubated the LB agar plates in oxalic conditions for two days at 20°C to allow *Penicillium* sp. laika to form a dense hyphal network that extends beyond the bacterial expansion range (Figure S1). We note that the cross-feeding bacterial pair engages in a competitive interaction for oxygen under oxalic conditions and generates patterns consistent with those generated by the competing pair under the same condition.<sup>15,72</sup> We then transferred the plates into a glove box (Coy Laboratory Products, Grass Lake, MI) filled with an anoxic nitrogen (N<sub>2</sub>):hydrogen (H<sub>2</sub>) (97%:3%) atmosphere at 20°C. After incubation in anoxic conditions for two additional days, which stopped growth of *Penicillium* sp. laika and promoted the anoxia-dependent interactions between the bacterial strains (competition or cross-feeding), the bacterial consortia had expanded across the fungal network to near the network's edge but without surpassing it. The intermixing indices measured at the expansion frontier therefore correspond to the anoxic growth period. We then removed the LB agar plates from the glove box and exposed them to ambient air for 1 h to promote maturation of the IPTG-inducible fluorescent proteins. We performed all experiments with five experimental replicates.

### Experimental procedure used to test the effects of active motility on bacterial range expansion

To test the mechanism driving bacterial dispersal along fungal hyphae, we performed range expansion experiments using *P. aeruginosa* PAO1-derived mutants that carry plasmid pBRM but either cannot generate functional type IV pili (strain PAO1- $\Delta$ *pilA-rfp*) or a functional flagellum (strain PAO1- $\Delta$ *fliC-rfp*) (Table S1). We additionally used the ancestral strain PAO1-*rfp* as a control. The experimental procedures are identical to those described above except that we mixed each strain individually with *Penicillium* sp. *laika* (i.e., these experiments contained only a single bacterial strain). We performed all experiments with five experimental replicates.

### Experimental procedure used to test for possible topographical effects caused by the fungal hyphae

To test whether the presence of fungal hyphae could create topographical effects that affect the maintenance of diversity during range expansion, we performed range expansion experiments using pairs of *P. aeruginosa* PAO1- $\Delta$ *fliC-rfp* and PAO1- $\Delta$ *fliC-gfp*. PAO1- $\Delta$ *fliC-gfp* carries plasmid pSMC21 that encodes for kanamycin resistance and green fluorescent protein (Table S1). The experimental procedures are identical to those described above. We performed all experiments with five experimental replicates.

### Experimental procedure used to test the effects of fungal hyphae on plasmid conjugation

To test whether fungal hyphae affect plasmid conjugation during range expansion, we introduced plasmid pAR145ecfp, which encodes for chloramphenicol resistance and cyan fluorescent protein, into *P. stutzeri* A1601-*egfp* by conjugation from the plasmid donor strain *Escherichia coli* DH5 $\alpha$  using conventional filter mating. This plasmid encodes for chloramphenicol resistance and cyan fluorescent protein and is self-transmissible (Table S1). We then quantified the extent of pAR145ecfp conjugation during range expansion in the absence or presence of fungal hyphae using the same strains and procedures as described above. We quantified the number of transconjugants that emerged during range expansion from confocal laser scanning microscopy (CLSM) images as described below. We performed all experiments with five experimental replicates.

### Confocal laser scanning microscopy

After completion of the range expansion experiments, we imaged the expansions directly on the agar plates without physically disturbing them using a Leica TCS SP5 II confocal laser scanning microscope (Leica Microsystems, Wetzlar, Germany) with a 5x HCX FL air immersion lens, a numerical aperture of 0.12, a frame size of 1024  $\times$  1024, and a pixel size of 3.027  $\mu$ m. We set the laser to 458 nm for the excitation of cyan fluorescent protein, to 488 nm for the excitation of green fluorescent protein, and to 514 nm for the excitation of red fluorescent protein.

### Scanning electron microscopy (SEM)

To perform SEM imaging of fungal-bacterial consortia, we first vapor fixed the consortia with 2.5% electron microscopy grade glutaraldehyde and 2% osmium tetroxide (OsO<sub>4</sub>) in distilled water. We then exposed the samples to glutaraldehyde for 90 minutes followed by OsO<sub>4</sub> for another 90 minutes. We next excised the vapor-fixed colonies from the plate, dried them in ambient air, and mounted the samples with conductive carbon cement onto SEM aluminium stubs. After outgassing overnight, we coated the samples with a 5 nm thick layer of platinum/palladium with rotation in a Safematic CCU-010 Metal Sputter Coater (LabTech, Hopkinton, MA, USA). Finally, we imaged the samples with a Shottky Field Emission Scanning Electron Microscope SU5000 (Hitachi High-Tech, Tokyo, Japan) at 2kV by secondary electron detection in collaboration with the Scientific Center for Optical and Electron Microscopy (ETH, Zürich, Switzerland) (<https://scopem.ethz.ch>).

## QUANTIFICATION AND STATISTICAL ANALYSIS

### Quantification of spatial intermixing

We quantified the magnitude of spatial intermixing (referred to as the intermixing index) between bacterial populations from the CLSM images.<sup>15,20</sup> The intermixing index provides a proxy measure of the number of individuals that emigrate from the inoculation area and contribute to active range expansion.<sup>7</sup> It can therefore be viewed as a proxy measure of diversity.<sup>15,20</sup> Briefly, if the initial population contains standing genetic diversity, then larger intermixing indices correspond with higher amounts of that initial standing genetic diversity that contribute to active range expansion.

An important challenge of analyzing spatial intermixing in range expansion experiments is to conserve as much information as possible. Loss of information derives from thresholding of images, which is necessary to count the number of transitions from one color to another. To minimize the loss of information, we developed a novel method that applies Fourier transforms across concentric rings at different expansion radii (Figure S6). This method does not binarize the data and conserves pixel-level signal intensities. We did this as follows. Starting with the original CLSM image (Figure S6A), we first extracted the layers that captured the strains expressing a given fluorescent protein (Figure S6B). We then extracted 1-pixel-wide rings at 3-pixel radial increments (Figure S6C) and transformed each ring into a sequence of  $\{\theta_i, px_i\}$ , where  $px_i$  is the value of the pixel that makes an angle of  $\theta_i$  with the positive x-axis direction (Figure S6D). We calculated the angles from the positive x-direction that originates at the center of the image and extends in the right direction. To accommodate for the circular periodicity of the data, we copied the data twice, shifted the values of the angles by  $2^*\pi$  and  $4^*\pi$ , and appended it to the original sequence. The length of the final sequence was therefore three times longer than the original one. We then performed Fourier transforms on the final sequence, whereby the resulting frequencies correspond to the

inverse of angles (Figure S6E). Each data point can be understood as how much mixing (Fourier amplitude) occurs with the corresponding frequency. In order to obtain the intermixing index at various length scales, we integrated the area under the curve of the Fourier transforms (Figure S6F). The dark grey area corresponds to intermixing at global scales (5 to 50 degrees), the blue area corresponds to intermixing at intermediate scales (0.5 to 5 degrees) and the red area corresponds to intermixing at local scales (0.2 to 0.5 degrees) (Figure S6F). We used local scales in this study because these scales match the pixel sizes at which we observed the finest scales of intermixing of different strains in our experiments.

In parallel, we also quantified the intermixing index for all of our experiments using a well-established intersection method.<sup>13</sup> To achieve this, we used a circular windowing approach to quantify the number of intersections between populations using Fiji (v1.53c) plugins (<https://fiji.sc>). Briefly, we first thresholded one of the color channels using the Huang algorithm implemented in ImageJ (<https://imagej.net>) and removed it from the image. We then removed remaining noise using the ‘remove outliers’ method (radius = 5, threshold = 50, bright). We next used the remaining 1-color image as an input to the Sholl plugin of ImageJ to calculate the number of intersections between background and information-containing parts of the image at 5  $\mu\text{m}$  increments from the outer edge of the inoculation area to the outer edge of the expansion frontier. For a measured number of intersections at a given radius ( $N_r$ ), we quantified the intermixing index ( $I_r$ ) as:

$$I_r = \frac{N_r}{\pi r/2}$$

We provided all of the intermixing indices calculated with the intersection method in the main figures or in Figure S3. Note that the intersection method resulted in the same qualitative conclusions as the local scale Fourier transform method.

For both the local scale Fourier transform and the intersection method, we accounted for unequal expansion sizes between biological replicates and treatments by transforming the radii to a relative scale (maximum radius set to one). After inspection of the trends of the intermixing index along the expansion radii, we removed the intermixing indices from the leading 2% of the expansion areas for all range expansions due to inadequate focus. Briefly, the thickness of the biomass becomes thinner towards the expansion frontier, which causes us to lose focus. We then defined the expansion frontier (*i.e.*, the actively growing layer of cells at the expansion edge) as a 35  $\mu\text{m}$  wide band at the expansion edge based on experimental measurements reported in a similar study.<sup>19</sup> This width corresponds to  $\sim 12$  cells assuming an average cell length of 2–3  $\mu\text{m}$ . The reported intermixing indices are the sum of the circumference-corrected intermixing indices at 5  $\mu\text{m}$  radial increments within the 35  $\mu\text{m}$  wide band.

### Quantification of plasmid pAR145ecfp transconjugants during range expansion

We quantified the number of transconjugants (*i.e.*, recipients that acquired plasmid pAR145ecfp) from the CLSM images. We first used functions implemented in Fiji (v1.53c) (<https://fiji.sc>) as described above for image preprocessing. We then counted the total number of overlapping blue and red pixels at 5  $\mu\text{m}$  radial increments from the outer edge of the inoculation area to the outer edge of the expansion frontier. We followed the same procedures to quantify the number of blue pixels only. We then divided the number of overlapping blue and red pixels (*i.e.* the number of transconjugants) by the number of blue pixels (*i.e.* the total number of potential recipients) at each radial increment. We next selected a radius of 350  $\mu\text{m}$  from the expansion edge as the region to statistically test the effects of fungal hyphae on the number of transconjugants. This is because this radius corresponds to the area where the effects of fungal hyphae on spatial mixing are quantifiable. We further estimated the total number of transconjugants in each range expansion by selective plating on LB agar plates amended with 30  $\mu\text{g ml}^{-1}$  chloramphenicol. For image presentation, we increased the intensity of the green channel. This caused the plasmid donors to appear as green and improved their visual differentiation from transconjugants.

### Quantification of biomass

We quantified the total biomass of individual range expansions by flow cytometry. We first used a spatula to detach and transfer the biomass from an entire range expansion into a 50 ml centrifuge tube containing 20 ml of phosphate-buffered saline solution and 1% potassium citrate. We then vortexed the solution for 10 minutes to fully suspend the cells and diluted the solution by 1000x (v:v). We next transferred 500  $\mu\text{L}$  of the solution into a 3.5 mL tube, added 5  $\mu\text{L}$  of SYBR Green, and incubated the tube in the dark for 10 min at 37°C. We then quantified the number of SYBR Green-labeled cells using a Accuri C6 flow cytometer (BD Accuri, San Jose, CA, USA) equipped with a 50 mW laser emitting at a fixed wavelength of 488 nm.<sup>73</sup> The flow cytometer was equipped with volumetric counting hardware and calibrated to measure the number of particles in a 50  $\mu\text{L}$  volume. We processed all data with the Accuri CFlow software (BD Accuri, San Jose, CA, USA) with electronic gating to separate bacterial-derived signals from instrument noise and sample background.

### Statistical analyses

We performed all statistical tests in the R software environment.<sup>69</sup> For each dataset, we tested for homoscedasticity with the Bartlett test and normality with the Wilk-Shapiro test. We assessed statistical significance between means of the fungal hyphae “Presence” and “Absence” factor levels using two-sample two-sided Welch tests implemented with the R core function *t.test* with unequal variances. We chose the Welch test because none of our datasets significantly deviated from normality but some significantly deviated from homoscedasticity. We reported the statistical test and the sample size for each test in the [results](#) section.